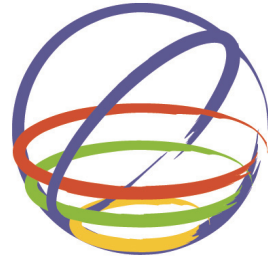


# Fractional derivatives: an alternative approach to model seismic wave attenuation and amplification



**L. Lenti**

*The French Institute of Sciences and Technology for Transport, Development and Networks (IFSTTAR), Université Paris Est, France, luca.lenti@ifsttar.fr*

**J.F. Nicolas**

*Ecole Polytechnique ParisTech, Department of Mechanics, Palaiseau, France*

**15 WCEE**  
LISBOA 2012

**F. Bonilla, J.F. Semblat**

*The French Institute of Sciences and Technology for Transport, Development and Networks (IFSTTAR), Université Paris Est, France*

**S. Martino**

*Department of Earth Sciences and Research Centre for Geological Risks (CERI)  
University of Rome, "La Sapienza", Italy*

**A. Rovelli**

*Istituto Nazionale di Geofisica e Vulcanologia, Rome, Italy*

## SUMMARY

Fractional derivations represent an efficient way of modeling the viscoelastic behavior of materials. This approach allows computing the current stress-strain conditions within a physical system by taking into account its stress-strain history. Here the fractional derivative is used to define the 1D viscoelastic constitutive law for dry soils. The parameters necessary to constrain the model are deduced from the estimated values of the damping ( $\alpha$ ), the shear modulus ( $G$ ) and the shear phase velocity at a reference frequency. The fractional-derivative-based model (FDRM) is then implemented in the frequency domain to characterize the 1D propagation of vertical SH waves under linear conditions ( $G$  and  $\alpha$  independent on the strain) and, by the use of an iterative scheme, under equivalent linear conditions ( $G$ ,  $\alpha$  vs. shear strains). The computed results (PGA and amplifications) are shown to be in good agreement with the results obtained from standard linear and linear equivalent approaches.

*Keywords:* Fractional derivatives, frequency-dependent rheology, numerical modeling, seismic amplification

## 1. INTRODUCTION

The so-called 'Fractional Calculus' is a topic of mathematics that gets off the more traditional assumptions at the basis of both the integral and the derivative calculus. Nowadays, fractional derivatives are considered to be a reliable methodology for describing the attenuation and dispersion of mechanic and electromagnetic waves in different typologies of materials, both man-made (i.e. rubbers, polymers) and natural (i.e rocks and soils) (Hilfer, 2000; Caputo, 1967; Caputo and Mainardi, 1971; Rocco et al., 1999; Machado et al., 2011; among many others). More generally, fractional-derivative-based calculus is adopted to describe the dynamic behavior of complex systems in many scientific applications, such as geophysics, biology, chemistry, astrophysics, social sciences (Metzler and Klafter, 2000; Saha-Ray and Bera, 2006). Among all these application, fractional derivatives represent a very useful tool for modeling seismic wave propagation in viscoelastic medium for which constant-Q models (i.e. based on a frequency independent attenuation) provide a reliable parametric characterization of the seismic attenuation within heterogeneous soils (Kjartansson \_1979; Emmerich and Korn, 1987; Carcione et al 1988; Day and Minister, 1995; Delepine et al., 2009). Fractional derivatives allow describing constant-Q rheologies without employing internal auxiliary memory variables as explained in the following; in this regard, Mainardi and Tomirotti (1997) interpreted the constant-Q model in terms of fractional derivatives and obtained the related 1D Green function. Fractional derivatives appear also in the Biot theory, related to memory effects in porous media. The

case of P- and S-wave propagation has been solved by Carcione et al., (2002) and by Carcione and Caputo (2011). In this work, fractional derivatives are used to define the 1D viscoelastic constitutive law for granular dry soils (such as silt, sands or granular moistures) as well as to model in the frequency domain the seismic wave propagation under strictly linear and linear-equivalent conditions. The two parameters needed for constraining the fractional rheological model are derived from the values of the damping ( $\alpha$ ), the shear modulus ( $G$ ) and the shear phase velocity at a reference frequency. As a first step an analytical analysis was carried on to compare the phase velocity functions associated to the here proposed model with the one related to the Kelvin-Voigt and the generalized Maxwell rheological models. As a second step, a 1D stress-strain path was output in the time domain by considering sinusoidal cyclic inputs at different frequencies and amplitudes in order to compare the so resulting decay curves (for both  $\alpha$  and  $G$ ) with the reference ones. The FDRM model was then implemented in the frequency domain to solve the upward propagation of SH waves within plane-parallel soil layers under both linear conditions (i.e.  $G$  and  $\alpha$  are independent on the strain level) and under equivalent linear conditions (i.e.  $G$ ,  $\alpha$  as a function of the shear strain level), in this case by performing an iterative solution. The results obtained in terms of transfer functions, PGA and response spectra are in good agreement with the ones obtained by applying more traditional linear and linear-equivalent approaches.

## 2. THE FRACTIONAL DERIVATIVE RHEOLOGICAL MODEL

The formulations of fractional derivatives proposed so far fall into two main groups: the Riemann-Liouville and Grunwald-Letnikov derivatives (Podlubny, 1999; Samko et al., 1993) and the Caputo derivatives (Caputo and Mainardi, 1971). Nevertheless, the Caputo derivative only guarantees that initial conditions can be expressed in terms of values of integer order derivatives (i.e. initial conditions considering values of velocities and displacements). In the following, the essential properties of the Caputo derivative are reported and only the fundamental features of the mathematical approach are here cited. The  $z$ -order Caputo derivative is defined by Eqn 2.1, where  $f(t)$ , null for  $t \leq 0$ , is at least an  $m$ -times derivable function respect to the time variable  $t$  with  $m \in \mathbb{N}_0$ ;  $f^m$  is the  $m$ th derivative of  $f(t)$ ;  $\Gamma$  is the gamma function reproducing the factorial function for integer argument;  $\xi$  is the integration variable and  $z$ , the fractional derivative order, which satisfies the condition  $m-1 \leq z \leq m$ .

$$\frac{d^z f(t)}{dt^z} = \frac{1}{\Gamma(m-z)} \int_0^t \frac{f^m(\xi)d\xi}{(t-\xi)^{z-m+1}} \quad (2.1)$$

For  $m=0$ , Eqn. 2.1 takes the form of Eqn. 2.2 where  $f^0(\xi) \equiv f(\xi)$  and  $-1 \leq z \leq 0$ . This form was adopted for the following application by assuming the  $z$ -order fractional derivative. A very important property of the above fractional derivative is shown through by Eqn. 2.3, which is obtained by taking the Laplace Transform ( $\mathcal{L}$ ) of the two members of Eqns 2.1-2.2.

$$\frac{d^z f(t)}{dt^z} = \frac{1}{\Gamma(-z)} \int_0^t \frac{f^0(\xi)d\xi}{(t-\xi)^{z+1}} \quad (2.2)$$

$$\mathcal{L}\left[\frac{d^z f(t)}{dt^z}\right] = (i\omega)^z \mathcal{L}[f(t)] \quad (2.3)$$

### 2.1. Definition of the rheological model

Starting from Lenti (2006), the 1D rheological model for the shear component of the strain and stress tensors (hereafter  $\varepsilon$  and  $\tau$  respectively) was here re-defined by adding the time function,  $t_0^z(z)$ ,

which represents the multiplicative material-dependent characteristic, and ensures that the solution of Eqn. 2.4 is properly dimensioned for any choice of the considered fractional order. The so re-defined function has the following formulation

$$\tau(t) = G t_0^{z+1} (z) \frac{d}{dt} \left[ \frac{d^z \varepsilon(t)}{dt^z} \right] = G t_0^{z+1} (z) \frac{d^{1+z} \varepsilon(t)}{dt^{1+z}} \quad (2.4)$$

From Eqn. 2.3 the Laplace transform of Eqn. 2.4 can be calculated as a function of the  $t$  variable, obtaining Eqn. 2.5 in the form:

$$T(\omega) = G t_0^{1+z} (i\omega)^{z+1} E(\omega) \quad (2.5)$$

where  $T$  and  $E$  are the Laplace transforms of the stress and strain shear components respectively,  $M(\omega) \equiv G t_0^{z+1} (i\omega)^{z+1}$  represents the complex modulus of the constitutive equation (Knopoff, 1964) which is expressed as a function of the circular frequency,  $\omega$ .

As  $M(\omega)$  has been defined, also the complex velocity -  $v(\omega)$ , the phase velocity -  $c(\omega)$ , and the attenuation factor -  $Q^{-1}$ , result to be defined according to the following Eqns 2.6-2.8 (Knopoff, 1964).

$$v(\omega) = \sqrt{M(\omega) / \rho} \quad (2.6)$$

$$c(\omega) = 1 / \operatorname{Re}(1/v(\omega)) \quad (2.7)$$

$$Q^{-1} \equiv 2\alpha = 2 \sqrt{\frac{\sqrt{\operatorname{Re}^2(M) + \operatorname{Im}^2(M)} - \operatorname{Re}(M)}{\sqrt{\operatorname{Re}^2(M) + \operatorname{Im}^2(M)} + \operatorname{Re}(M)}} \quad (2.8)$$

where  $\rho$  is the density of the material, “Re” and “Im” indicate the real and the imaginary part of complex functions respectively and  $\alpha$  is the damping.

### 2.1.1. Determination of the fractional derivative parameters

The fractional derivative order ( $z$ ) can be deduced from Eqns 2.5 to 2.8 as a function, expressed in the following Eqn. 2.9, of the damping value only.

$$z = \frac{2}{\pi} \arccos \left( \frac{1-\alpha^2}{1+\alpha^2} \right) - 1 \quad (2.9)$$

The value of the shear modulus ( $G$ ) is assumed so to guarantees that an elastic condition (i.e.,  $\alpha=0$ ) results for  $z$  equal to -1 in Eqns 2.4-2.8.

The phase velocity related to the model is deduced from Eqns 2.5 and 2.7 and expressed by Eqn. 2.10 in the form:

$$c(\omega) = \frac{c_0}{\cos \left( \frac{\pi}{4} (1+z) \right)} (t_0 \omega)^{\frac{1+z}{2}} \quad (2.10)$$

where  $c_0 = \sqrt{G/\rho}$  is the elastic frequency-independent phase velocity. Eqn 2.10 allows fixing the  $t_0$  value when the velocity phase at a reference frequency is known. With no loss of generality, we consider the phase velocity at 1 Hz ( $\omega_0=2\pi$ ) equal to  $c_0$ . From Eqn 2.10 we then deduce Eqn 2.11 in the form:

$$t_0 = \frac{1}{\omega_0} \left( \cos \left( \frac{\pi}{4} (1+z) \right) \right)^{\frac{2}{1+z}} \quad (2.11)$$

**Table 2.1.** Shear modulus ( $G$ ), damping ( $\alpha$ ), density and reference phase velocity values for the here considered materials which were used to compute the values of the rheological parameters  $z$  and  $t_0$  according to Eqns. 2.9 and 2.11.

Type of soil	Density (kg/m <sup>3</sup> )	$G$ (MPa)	$\alpha$ (%)	Phase vel. 1Hz (m/s)	Derivate order ( $z$ )	$t_0$ (sec)
Soil_1	1900	116	5	241	-0.9364	0.1530
Soil_2	2000	612	1	540	-0.9873	0.1579
Rock	2100	20000	0.1	3086	-0.9987	0.1590

The above reported Eqns were here applied to 3 different natural materials (including soils and rock) as reported in Table 2.1. In particular, for each considered soil the values of  $G$ ,  $\alpha$ , density and phase velocity are supposed to be known at 1Hz allowing computing the related values of the derivative order ( $z$ ) and of the characteristic time ( $t_0$ ).

### 2.1.2. Phase velocity and attenuation curves for the fractional model

According to the fractional model (FDRM) represented by Eqns 2.9 and 2.10 the attenuation factor and phase velocity curves can be plot as a function of frequency for the soils reported in Table 2.1. In Figure 1, the so derived curves are compared with the ones calculated according to the Kelvin-Voigt (Kramer, 1996) and to the generalized Maxwell Body (MB) models respectively (Emmerich and Korn, 1987). All the curves were derived by assuming that the phase velocity value is known at 1Hz. The phase velocity functions for the FDRM are in very good agreement with the values related to the MB model (for the MB model in this work we considered 3 internal variables and 0.1, 1 and 10Hz as calibrating frequencies).

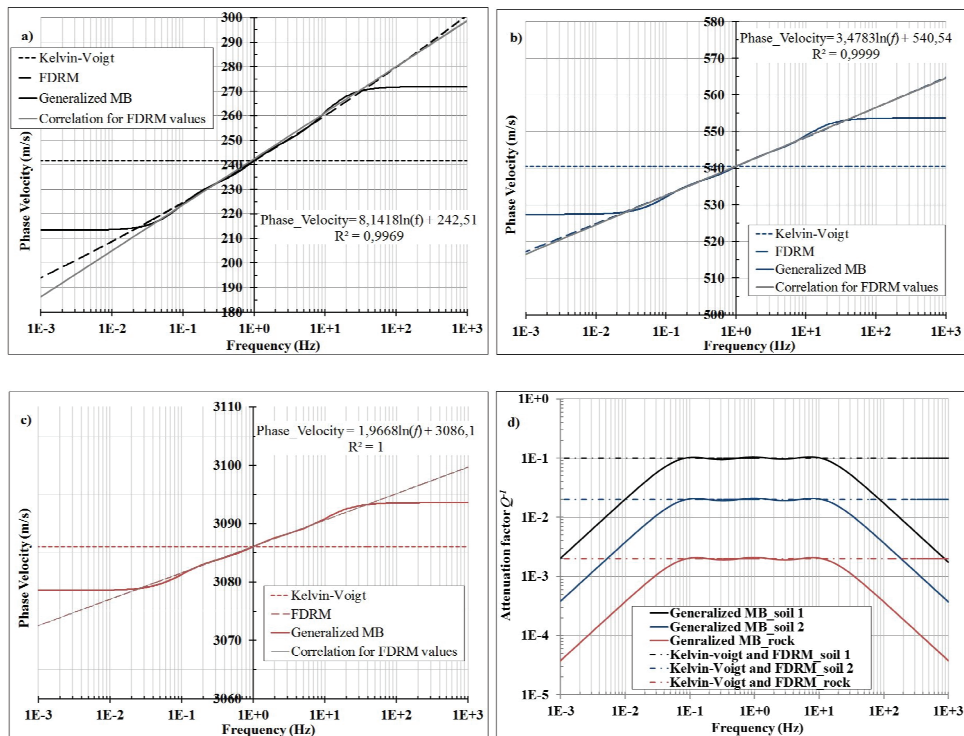


**Figure 1.** Comparison among phase velocity functions calculated considering the Kelvin-Voigt, the MB and the FDRM for the soil 1 (a), 2 (b) and the rock (c) of Table 2.1 (linear correlation functions and related  $R^2$  values are also reported for the phase velocity functions of the FDRM values); d) comparison among the attenuation factors related to the here considered materials and the different rheologies.

In particular, the phase velocity values related to the FDRM show a quasi-linear trend vs.  $\ln(f)$  over the whole frequency domain (see in Figure 1 the related linear correlation functions), allowing to consider the FDRM reliable in taking into account dispersion phenomena (Aki and Richards, 1980). On the other hand, the attenuation factor for the Kelvin-Voigt and the FDRM do not vary over the entire frequency domain.

## 2.2. Shear stress-strain paths

To analyze the results of the here proposed fractional-derivative rheological model, we consider sinusoidal shear strain inputs at different frequencies (from 0.1 to 10Hz) and at various amplitudes (from  $10^{-6}$  to  $10^{-1}$ ) to compute shear strain-stress paths in the time domain according to Eqn 2.4. The shear modulus ( $G$ ) and the damping ( $\alpha$ ) are chosen for each amplitude considering the curves plotted on Figure 2b and 2c (solid lines) respectively, and giving as initial shear modulus ( $G_0$ ) the value of 185MPa. For every couple of values  $G$  and  $\alpha$ , the FDRM parameters (the derivative fractional order and the characteristic time) are deduced from Eqns 2.9 and 2.11 respectively, assuming the phase velocity at 1Hz given by  $c_0 = \sqrt{G/\rho}$ . In Figures 2d, 2e and 2f three examples of paths are computed for three different sinusoidal amplitudes at 1Hz, adopting our model (blue line) as well as the Kelvin-Voigt model (red line). A good agreement is found from this comparison in terms of shapes of cycles but, despite the Kelvin-Voigt cycles, the ones obtained by the fractional approach are characterized by initial null values of the stress if initial null values of the strain are assumed. In order to take into account the frequency dependence of the FDRM the equivalent parameters (secant  $G$  and  $\alpha$ ) related to the computed cycles and computed according to the sketch on Figure 2a, were analyzed as a function of frequency. The obtained results are shown in Figures 2b and 2c respectively and demonstrate a non-negligible role of frequency on the shape of the  $G$  curves (with relative differences up to 50%).

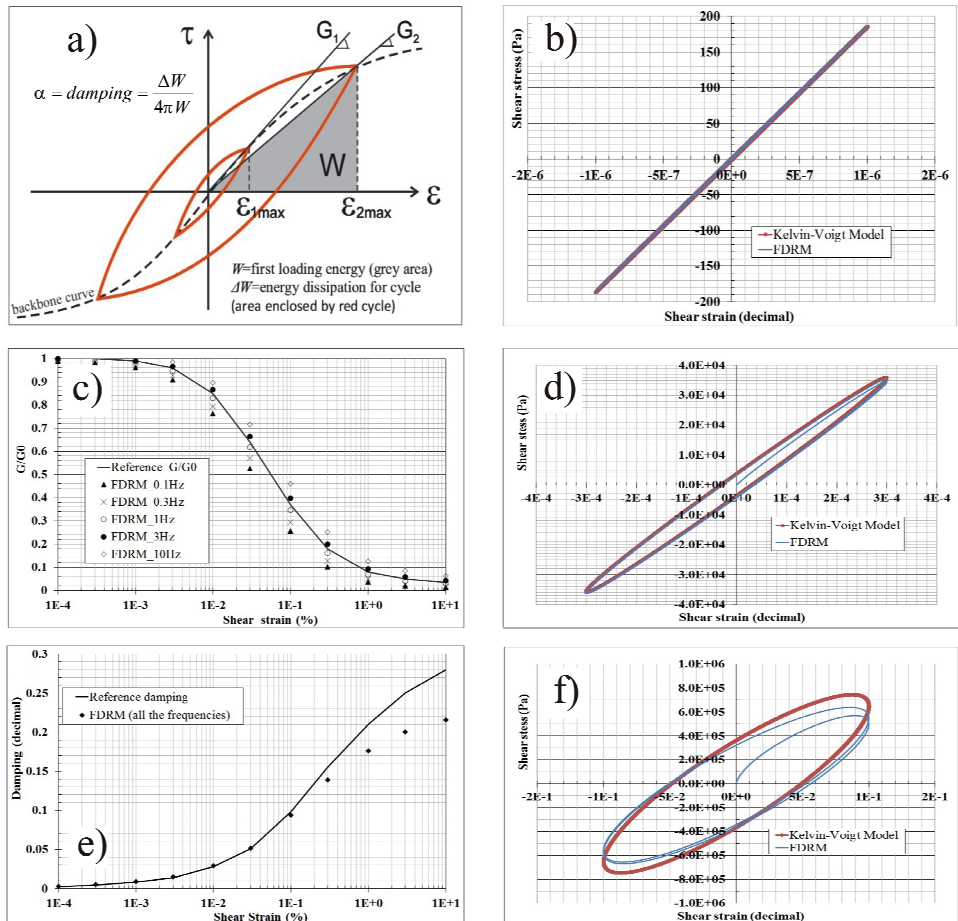


**Figure 2.** a) Qualitative sketch of hysteresis cycle with damping ( $\alpha$ ) and secant modulus ( $G$ ) definitions; comparisons between reference curves and curves obtained by the FDRM (in the case FDRM the variability of the curves over frequency is also considered) for the shear modulus reduction curves (b) and for the damping curves (c) respectively; d), e) and f) comparisons between hysteresis cycles obtained adopting the Kelvin-Voigt and the FDRM for 3 shear strain levels reached by sinusoidal inputs at different amplitude.

This variability is the result of the described quasi-linear dependence of the phase velocity vs.  $\ln(f)$ . In particular, the computed reduction curves which present minor relative differences with respect to the reference modulus reduction curve are related to the results obtained considering the sinusoids at 1 and 3Hz. This effect is a consequence of the particular choice made to fix the value of the phase velocity at 1Hz (see Eqn 2.10). However, similar qualitative features can be found assuming other values for the phase velocity at a given frequency. Conversely, the obtained damping curves are frequency-independent as a consequence of the analytical independence of the fractional order on frequency expressed by Eqn 2.9. A higher coincidence between the FDRM calculated  $\alpha$  curves and the reference one results for strain amplitudes up to  $10^{-3}$  (relative errors < 1%); the difference gradually increases up to 25%, for a strain level of  $10^{-1}$ .

### 3. 1D SEISMIC WAVE PROPAGATION IN THE FREQUENCY DOMAIN

The here proposed FDRM was implemented by a Fortran95 code aiming at simulating, both under linear and equivalent linear conditions (Kramer, 1986), the propagation of vertical upward SH waves. The results obtained by the FDRM are here presented in comparison with the ones obtained by applying the classical linear equivalent approach (Schnabel et al., 1972).

At this aim the layering reported on Figure 3a was considered where  $x$  represents the vertical direction and  $u$  the horizontal displacement along the  $y$  direction. Adopting the same formalism introduced in the previous section, for each layer the dynamic equilibrium and the initial and boundary conditions are expressed by Eqns 3.1 and Eqns 3.2 respectively ( $t_m$  and  $t$  are in the order the characteristic time for the  $m$ th layer and the time variable).

$$\begin{cases} \rho_m \frac{\partial^2 u_m(t)}{\partial t^2} = \frac{\partial \tau_m(t)}{\partial x_m} \\ \tau_m(t) = G_m t_m^{1+z_m}(z) \frac{\partial^{1+z_m} \mathcal{E}_m(t)}{\partial t^{1+z_m}} \end{cases} \quad (3.1)$$

$$\begin{cases} u_m(x_m, t=0) = 0 \\ \frac{\partial u_m(x_m, t=0)}{\partial t} = 0 \\ \frac{\partial u_1(x_1=0, t)}{\partial x_1} = 0 \\ u_m(x_m = h_m, t) = u_{m+1}(x_{m+1}=0, t) \\ \tau_m(x_m = h_m, t) = \tau_{m+1}(x_{m+1}=0, t) \end{cases} \quad (3.2)$$

The Laplace transform of the first of Eqns 3.1 is represented by Eqn 3.3 where  $i$  is the imaginary unit,  $U_m$  and  $U_{m,xx}$  are the temporal Laplace transforms of the displacement and of the second derivative of the displacement respect to the  $x$  direction respectively.

$$\begin{cases} U_m(\omega) + \frac{1}{\omega_m^2} U_{m,xx}(\omega) = 0 \\ \omega_m^2 \equiv \frac{\rho_m \omega^2}{G_m t_m^{1+z_m} i^{1+z_m} \omega^{1+z_m}} \end{cases} \quad (3.3)$$

The general solution of Eqn 3.3 can be expressed by Eqn 3.4 where  $A_m$  and  $B_m$  are in the order the spectral amplitude of the incidence and reflecting waves. The continuity of the shear strain and stress components between 2 adjacent layers is expressed, in the frequency domain, by Eqns 3.5.

$$U_m(\omega) = A_m e^{i\omega_m x_m} + B_m e^{-i\omega_m x_m} \quad (3.4)$$

$$\begin{cases} A_{m+1} = \frac{1}{2} [A_m e^{iw_m h_m} (1 + \gamma_{m,m+1}) + B_m e^{-iw_m h_m} (1 - \gamma_{m,m+1})] = a_{m+1}(\omega) A_i \\ B_{m+1} = \frac{1}{2} [A_m e^{iw_m h_m} (1 - \gamma_{m,m+1}) + B_m e^{-iw_m h_m} (1 + \gamma_{m,m+1})] = b_{m+1}(\omega) A_i \\ \gamma_{m,m+1} = \left( \frac{\rho_m G_m}{\rho_{m+1} G_{m+1}} \right)^{1/2} e^{\frac{i\pi(z_m - z_{m+1})}{4}} t_m^{1/2} t_{m+1}^{1/2} \omega^{-2} \\ A_i = B_i \end{cases} \quad (3.5)$$

In Eqns 3.5 the functions  $a_{m+1}(\omega)$  and  $b_{m+1}(\omega)$  can be solved iteratively considering  $A_i=B_i=1$ . Their knowledge allows describing the transfer function (TF) between two layers selected within the soil column. In particular, considering the first and the  $N$ th layer we have the Eqn 3.6 and, for the transfer function between the first layer and the outcropping bedrock ( $N'$ ) the Eqn 3.7.

$$\frac{U_1}{U_N} = \frac{2}{a_N + b_N} \quad (3.6)$$

$$\frac{U_1}{U_{N'}} = \frac{1}{a_N} \quad (3.7)$$

### 3.1. Seismic wave propagation under linear conditions

Seismic wave propagation was also exemplified under linear conditions by adopting the same layering in Figure 3a, and by applying an acceleration time-history considered on the outcropping bedrock, as reported in Figure 3b; in this case the system is considered to be composed by 2 layers over a viscoelastic substratum whose properties are reported in Table 3.1.

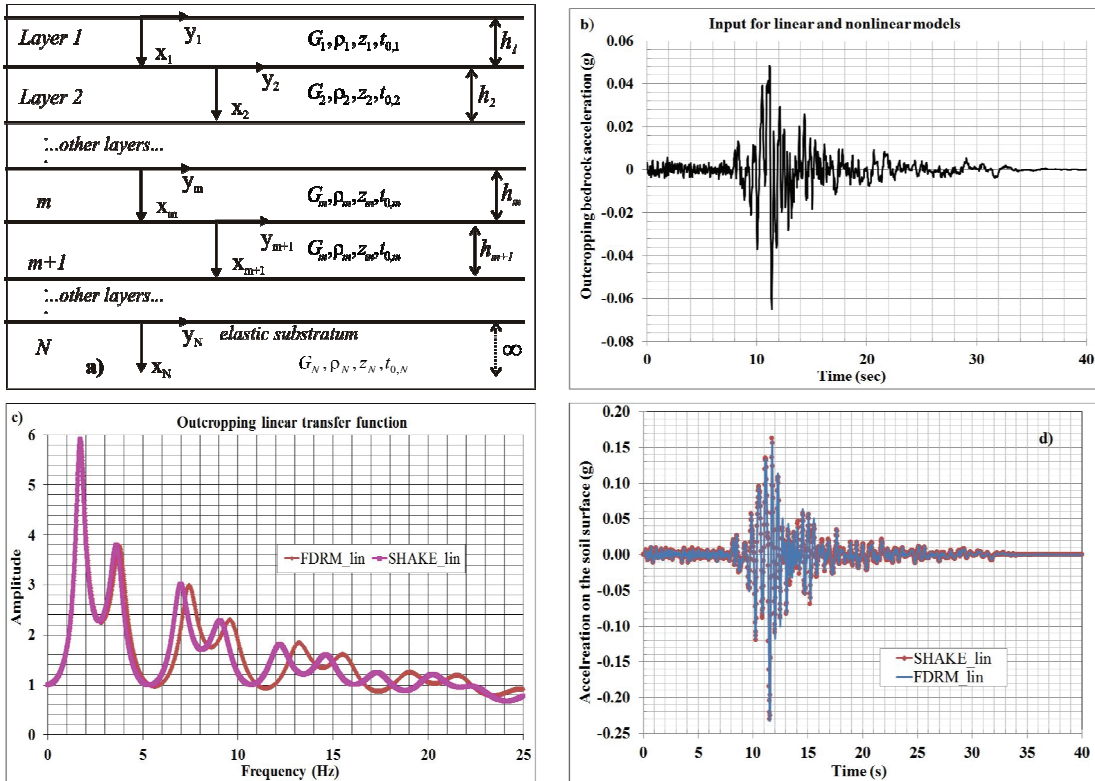


**Figure 3.** a) Qualitative sketch of the here considered plane-parallel layering ( $x$  and  $u$  are the vertical direction and the horizontal displacement respectively); (b) acceleration time history of the outcropping bedrock adopted for the linear and linear-equivalent modeling (Loma Prieta Earthquake, recorded at Yerba Buena Island, available from the EDUSHAKE dataset); comparison between the TFs (c) and surface acceleration time histories (d) related to the FDRM approach and to SHAKE computational code under linear conditions.

Also in this case the problem was solved by adopting the here proposed FDRM approach and by using the linear-equivalent approach by using the code SHAKE under a linear assumption (i.e. by performing only 1 computational step).

Figure 3 shows the resulting outputs in terms of comparison between the Transfer Function (TFs) computed from the bottom and the outcropping layer.

This comparison demonstrates that the TFs are characterized by the same frequency-peaks and amplitude in the range 0-5Hz. Also the modeled time histories are quite equivalent, as proved by a relative difference of the resulting PGAs less than 0.5%. On the contrary, at higher frequency values, the TF amplitude modeled by the two approaches coincide but the TF peak result at different frequency values, since higher modes are rightward shifted in the case of FDRM approach as a functional effect of the frequency-dependent FDRM.

**Table 3.1.** Shear modulus ( $G$ ), damping ( $\alpha_0$ ), thickness and density values for the here considered layering (see Fig.3) in case of seismic wave propagation under linear conditions; the derivative fractional order ( $z_0$ ) and the characteristic time ( $t_0$ ) are deduced from Eqns 2.9 and 2.11 respectively, considering  $(G_0/\rho)^{0.5}$  as known value of the phase velocity at 1Hz.

Type of soil	$G_0$ (MPa)	$\alpha_0$ (%)	Thickness (m)	Density (kg/m <sup>3</sup> )	Deriv. order ( $z_0$ )	$t_0$ (sec)
Layer 1	171	5	30	1900	-0.9363	0.1530
Layer 2	1000	2	60	2000	-0.9745	0.1579
Rock	20000	0.5	$\infty$	2100	-0.9936	0.1590

### 3.2. Seismic wave propagation under linear-equivalent conditions

A linear-equivalent approach was implemented according to the here proposed FDRM approach by a Fortran95 formulation. More in particular, the iterative procedure implemented for simulating the 1D seismic wave propagation according to the here proposed FDRM approach follows the same numerical formulation adopted by SHAKE (Schnabel et al., 1972) by substituting the Kelvin-Voigt rheology with the FDRM one.

More in particular, the same solution of SHAKE code were here adopted for computing the effective shear strain as well as the convergence error related to two successive iterations (this last one used for stopping the iterative procedure). For performing the linear-equivalent numerical experiment, a 2 layer over viscoelastic bedrock soil column was considered whose thicknesses are reported in Table 3.1. The initial, low strain  $G$  and  $\alpha$  values as well as the related initial  $z_0$  and  $t_0$  values are also reported in Table 3.1. The applied time history is reported in Figure 3b. The curves in Figure 4a are considered to take into account the modulus reduction and the damping increasing. The results obtained in terms of time history on the soil column top, response spectrum, and TF are reported in Figure 4 by comparing the outputs by SHAKE and by adopting the FDRM approach. The FDRM modeled time-histories are generally characterized by values lower than the ones resulting by SHAKE computational code; in particular, the relative difference on the PGA is of about 19%. Moreover, also in this case, the resulting TFs are characterized by the same frequency-peaks and amplitudes in the frequency range 0-5Hz (i.e. relative difference referred to the resonance peak lower than 6%). On the contrary, at higher frequencies, the FT amplitudes are similar, but the resonant frequencies are different by applying the 2 rheologies since, in the case of the frequency-dependent FM approach the highest modes (>5Hz) are rightward shifted of about 20%.

Analogous results were obtained in terms of response spectra, as reported in Figure 4d, since, also in this case, non-negligible differences between the SHAKE solution and the FDRM one are output for period higher than 0.2 sec. As a further result, the time-distribution of seismic wave was checked by the spectrograms reported in Figures 4e and 4f in order to point out possible relation with the phase velocities; nevertheless, the obtained results show no significant differences in the arriving order of the frequencies. However, it is worth noticing that the input signal here considered is related to the Mw 6.9 earthquake of Loma Prieta, 1989, which is characterized by a very low spectral content for frequencies higher than about 4Hz. The influence of the phase velocity on the frequency for broadband signals is a topic of on-going researches by the Authors. These analyses should clarify the aspect of dependence of the phase velocity and its consequences that can be of specific interest for solving numerical modeling seismic wave propagation under 2D and/or 3D conditions, i.e. if the dispersion of the surface seismic waves becomes a more significant phenomenon to be considered.

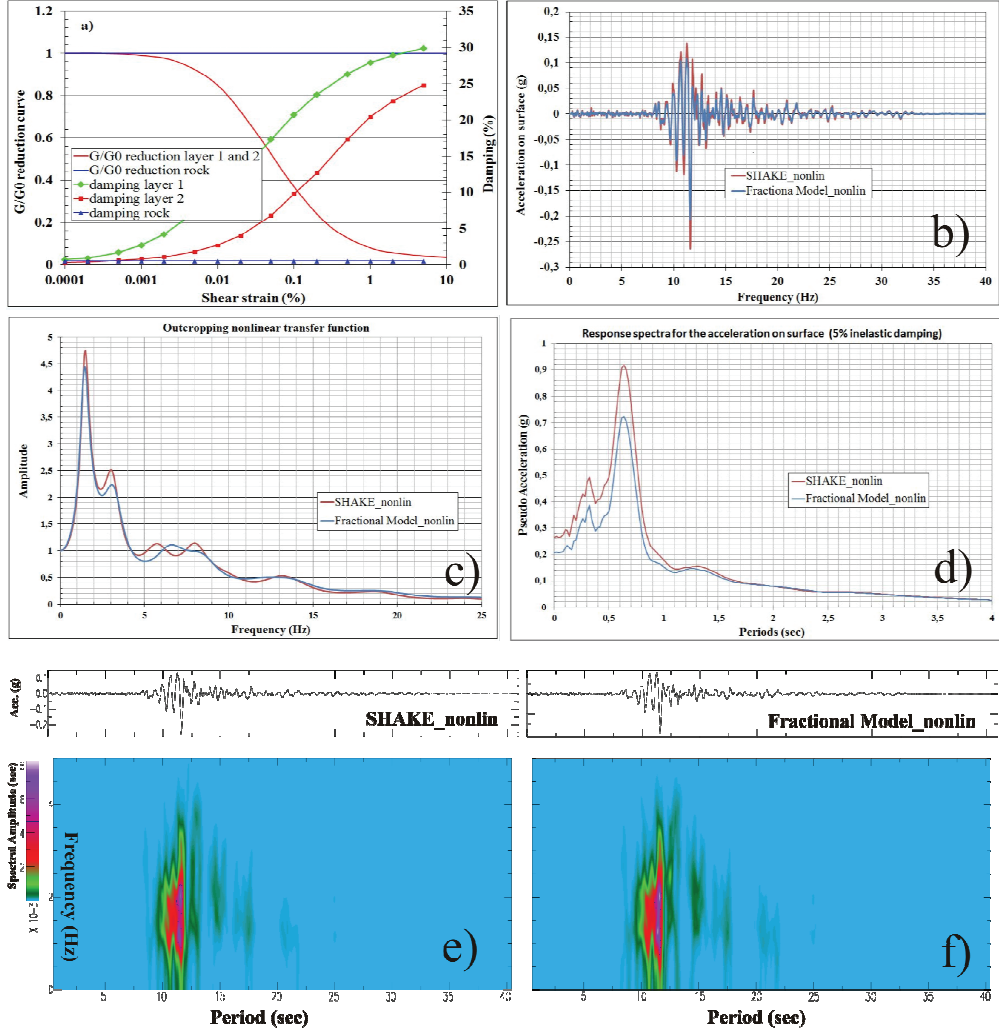


**Figure 4.** Comparisons between the results obtained by the FDRM and SHAKE computational code under linear-equivalent conditions: a) reference G and  $\alpha$  decay curves; b) acceleration time histories at soil column top; c) outcropping TFs; d) response spectra at soil column top; e) spectrogram of the output time-histories modeled at the soil column top in the case of SHAKE computational code (1s sliding window with slice time 0.1 sec); f) spectrogram of the output time-histories modeled at the soil column top in the case of the FDRM approach (1s sliding window with slice time 0.1 sec).

#### 4. CONCLUSIONS

The Caputo fractional-derivative-based approach was here considered as a mathematical tool to stress-strain modeling of the viscoelastic rheological behavior, as well as to simulate 1D seismic wave propagation aiming at inferring on the local seismic response of a plane-parallel dry-soil layering. The here proposed FDRM approach needs only 2 parameters, i.e., the material characteristic time ( $t_0$ ) and the fractional derivative order ( $z$ ), to be derived from three basic rheological parameters of the considered soil, i.e. the shear modulus  $G$ , the damping factor  $\alpha$  and the phase velocity at a reference frequency. Since the phase velocity, considered in the FDRM approach, is frequency-dependent it allows taking into account dispersion phenomena. As it results from this condition, the hysteretic cycles obtained with the FDRM are characterized by a more realistic shape showing null values of stress if null values of strain are imposed as initial conditions. The modulus reduction curves obtained from the computed cycles are frequency dependent. The FDRM rheological approach was also implemented by a computational solution in the frequency domain to perform seismic wave propagation to assess the site response of a soil column under both linear (viscoelastic) and linear equivalent (hysteretic) conditions. The obtained results demonstrate that the FDRM provide TFs

which show more relevant differences with respect to the ones obtained by adopting the Kelvin-Voigt model (i.e. implemented by the common computational code SHAKE) at higher frequencies (both in terms of TF frequency peaks and related amplitudes) as an effect of the functional frequency-dependence due to the FDMR approach. Further analyses are needed to better evaluate the effects of the frequency dependence on the arriving order of frequencies in the case of signals with non-negligible spectral content at higher frequencies. This kind of analysis becomes essential for simulating seismic wave propagation in 1D condition if angulated incidences are considered, as well as in case of 2D and 3D conditions, i.e. where soil heterogeneities are responsible for generation of surface waves. As a final consideration, since the ground-motion which is modeled at the building foundations actually result by the cumulative effect due to different components of the seismic waves, a better theoretical modeling of the seismic wave propagation, in terms of both attenuation and dispersion phenomena, constitutes an useful tool for providing more robust evaluations of the expected ground-motion, which can be reliable for civil engineering designs with respect to seismic actions.

## REFERENCES

- Aki, K. and Richards, P. G. (1980). Quantitative seismology. Theory and Methods. W. H. Freeman and Company, San Francisco, USA.
- Caputo, M. (1967). Linear models of dissipation whose Q is almost frequency independent, II. *Geophys. J. Royal Astronom. Soc.*, 529-539.
- Caputo, M., and F. Mainardi, (1971). Linear models of dissipation in anelastic solids. *Il Nuovo Cimento, Ser. II*, 1, 161–198.
- Carcione, J. M., Kosloff, D. and Kosloff, R. (1988). Wave propagation simulation in a linear viscoelastic medium. *Geophysical Journal of the Royal Astronomical Society*, 95, 597–611.
- Carcione, J. M., Cavallini, F., Mainardi, F. and Hanyga, A. (2002). Time-domain seismic modeling of constant Q-wave propagation using fractional derivatives. *Pure and Applied Geophysics*, 159:7, 1719–1736.
- Carcione, J. M. and Caputo, M. (2011). Wave simulation in dissipative media described by distributed-order fractional time derivatives. *Journal of Vibration and Control*, 17:8, 1121–1130.
- Day, S. M. and Minister, J. B. (1984). Numerical simulation of attenuated wavefields using a Padé approximant method, *Geophys. J. R. Astr. Soc.*, 78, 105-118.
- Delapine, N., Lenti, L., Bonnet, J., Semblat, JF. (2009). Nonlinear viscoelastic wave propagation: an extension of Nearly Constant Attenuation (NCQ) models. *Jal of Engineering Mech. (ASCE)*, 135:11, 1305-1314.
- Emmerich, H. and Korn, M. (1987). Incorporation of attenuation into time-domain computations of seismic wave fields, *Geophysics*, 52, 1252-1264.
- Hilfer R. (2000). Applications of Fractional Calculus in Physics, World Scientific Publishing Co.
- Kjartansson, E. (1979). Constant Q-Wave Propagation and Attenuation. *Journal of Geophysical Research*, 84 no. B9, 4737-4748, doi:10.1029/JB084iB09p04737.
- Kramer, S. L. (1996). Geotechnical Earthquake Engineering. Prantice Hall, Upper Saddle River, New Jersey 07458, pp. 653.
- Knopoff, L. (1964). Q. *Rev. Geophys.*, 2, 625–660.
- Lenti, L. (2006). Modellazione di effetti non lineari in terreni soggetti a carico ciclico e dinamico. PhD. thesis, Università di Bologna “ALMA MATER STUDIORUM”, 06/2006.
- Machado, J. T., Kiryakova, V. and Mainardi F. (2011). Recent history of fractional calculus. *Communications in Nonlinear Science and Numerical Simulation*, 16:3, 1140-1153.
- Mainardi, F. and Tomirotti, M. (1997). Seismic pulse propagation with constant and stable probability distributions. *Annali di Geofisica*, 40, 1311–1328.
- Metzler, R. and Klafter, J. (2000). The random walk's guide to anomalous diffusion: a fractional dynamics approach. *Physics Reports*, 339:1, 1-77.
- Podlubny, I. (1999). Fractional differential equations. Academic Press, New York.
- Rocco, A. and West, J.B. (1999). Fractional Calculus and the evolution of fractal phenomena. *Physica* 265, 535-546.
- Saha-Ray, S. and Bera, R. K. (2006). Analytical solution of a fractional diffusion equation by Adomian decomposition method. *Applied Mathematics and Computation*, 174:1, 329-336.
- Samko, S., Kilbas, A. and Marichev, O. (1993). Fractional Integrals and Derivatives: Theory and Applications. Gordon and Breach, London.
- Schnabel, Per B., Lysmer, J. and Seed, H. B. (1972). SHAKE: a computer program for earthquake response analysis of horizontally layered sites. UCB/EERC-72/12, Earthquake Engineering Research Center, University of California, Berkeley, 12, 92 pages (480/S36/1972).